

1 of 1

**PROGRESS REPORT  
ON  
RESEARCH IN NUCLEAR PHYSICS**

**July 1, 1992 - May 31, 1993**

**R. L. Kozub and M. M. Hindi**

**DISCLAIMER**

This report was prepared as an account of work sponsored by an agency of the United States Government. Neither the United States Government nor any agency thereof, nor any of their employees, makes any warranty, express or implied, or assumes any legal liability or responsibility for the accuracy, completeness, or usefulness of any information, apparatus, product, or process disclosed, or represents that its use would not infringe privately owned rights. Reference herein to any specific commercial product, process, or service by trade name, trademark, manufacturer, or otherwise does not necessarily constitute or imply its endorsement, recommendation, or favoring by the United States Government or any agency thereof. The views and opinions of authors expressed herein do not necessarily state or reflect those of the United States Government or any agency thereof.

**DEPARTMENT OF PHYSICS  
TENNESSEE TECHNOLOGICAL UNIVERSITY  
COOKEVILLE, TENNESSEE 38505**

**June, 1993**

**PREPARED FOR THE U. S. DEPARTMENT OF ENERGY  
UNDER GRANT NUMBER DE-FG05-87ER40314**

**MASTER**

**DISTRIBUTION OF THIS DOCUMENT IS UNLIMITED**

## CONTENTS

Preface	1
Search for Massive Neutrinos in the Recoil Spectrum of $^{37}\text{Cl}$ following Electron Capture Decay of $^{37}\text{Ar}$	2
A Monte Carlo Simulation of the Electron Capture Decay of $^{37}\text{Ar}$ with an Admixture of Massive Neutrinos	7
Search for 17-keV Neutrinos in the Internal Bremsstrahlung Spectrum of $^{125}\text{I}$	10
$\beta^+$ Decay and Cosmic-Ray Half-Lives of $^{143}\text{Pm}$ and $^{144}\text{Pm}$	17
Production Cross Sections from the Bombardment of Natural Mo with Protons	22
Publications and Seminars	30
TTU Personnel	33
Appendix:	
Yrast Decays in $^{43}\text{K}$ (reprint)	
$\beta^+$ Decay and Cosmic-Ray Half-Life of $^{91}\text{Nb}$ (preprint)	

## PREFACE

The progress on Grant No. DE-FG05-87ER40314 from July 1, 1992 to May 31, 1993, is summarized in this report. The main emphases of the program are studies of the structure of neutron-rich nuclei and rare electron capture processes.

Most of our activities for the past year were centered on the rare electron capture component of our program, using experimental facilities at Tennessee Technological University (TTU) and Montana State University (MSU). In addition, experiments of astrophysical significance were conducted at Lawrence Berkeley Laboratories (LBL). Our proposed research on neutron-rich nuclei requires the Fragment Mass Analyzer (FMA) at the Argonne Tandem-Linac Accelerator System (ATLAS), an array of Compton-suppressed Ge detectors, and a detector capable of identifying atomic numbers of fragments reaching the FMA focal plane. Such a combination has not yet been available for use.

Four undergraduate students, all majoring in physics, are currently working on the project. They are Alex Altgilbers, Danny Bardayan, Brian Faircloth, and Predrag Miočinović. All are working diligently and making positive contributions.

The secretarial and accounting duties for this project have again been performed expertly by Gloria Julian. We appreciate her efficient, accurate service and unwavering self control.

We would like to thank the many scientists and support personnel at other institutions and laboratories who have assisted us with this work. In particular, MMH is deeply appreciative of the hospitality and support shown him during his visits to LBL and MSU.

Finally, we would like to remind the reader that the work described in this report is preliminary and should not be quoted in the literature without prior permission.

R. L. Kozub

M. M. Hindi

## Search for Massive Neutrinos in the Recoil Spectrum of $^{37}\text{Cl}$ following Electron Capture Decay of $^{37}\text{Ar}$

M.M. Hindi, R.L. Kozub, S.J. Robinson, R. Avci,<sup>†</sup> Lin Zhu,<sup>†</sup> and G. J. Lapeyre<sup>†</sup>

We are developing an experiment to measure the spectrum of recoil velocities of  $^{37}\text{Cl}$  ions following the electron capture (EC) decay of  $^{37}\text{Ar}$ . One of the initial aims of this experiment is to search for massive neutrinos ( $m \approx 200\text{--}250$  keV) which might be emitted in the decay. The current direct limit on the mass of the muon neutrino is  $m_{\nu_\mu} < 250$  keV;<sup>1</sup> the limits on its mixing with the electron neutrino deduced from the  $\beta^+$  and  $\beta^-$  decay of  $^{64}\text{Cu}$  is  $< 0.5\%$  for  $m = 200$  keV,<sup>2</sup> and from  $\nu_\mu \rightarrow \nu_e$  appearance experiments at accelerators<sup>3</sup> the limit is  $< 0.34\%$  for large  $\Delta m^2$ . We hope to improve on these limits.

The principle of the experiment is simple: an atomic monolayer of  $^{37}\text{Ar}$  ( $t_{1/2} = 35$  d) will be deposited on a cooled silicon crystal in an ultrahigh vacuum (UHV) system. The  $^{37}\text{Ar}$  atom decays by EC into a  $^{37}\text{Cl}$  atom and a neutrino. Energy and momentum conservation then dictate that the  $^{37}\text{Cl}$  atom recoil with a fixed velocity ( $v = 0.71 \text{ cm}/\mu\text{s}$ ,  $E = 9.54 \text{ eV}$ ). If a heavy neutrino is emitted, the recoil velocity is smaller by 3.1–4.9% for  $m_\nu = 200\text{--}250$  keV. The recoil velocity can be measured by starting a time-to-amplitude (TAC) converter on x rays or Auger electrons emitted in filling the hole left in the atom after orbital electron capture, and stopped by detecting the positively charged recoiling  $^{37}\text{Cl}$  ion after it travels a distance of several centimeters. A Monte Carlo simulation of the time of flight spectrum which takes into account the effect of the initial thermal velocity of the  $^{37}\text{Ar}$  atom and of the recoil from Auger emission of the daughter  $^{37}\text{Cl}$  ion has been conducted and is described elsewhere in this report. Here we describe the experimental progress achieved so far.

$^{37}\text{Ar}$  was produced via the  $^{36}\text{Ar}(n, \gamma)^{37}\text{Ar}$  reaction. A quartz ampoule filled with 10 ml of  $^{36}\text{Ar}$  enriched to 99.5 atom % was purchased from Isotec Inc., and irradiated for one week at the Brookhaven National Laboratory reactor. At the end of irradiation the source strength was approximately 300 mCi. The source was shipped to the Physics Department at Montana State University where all the measurements described here were conducted.

The ampoule was introduced into a vacuum chamber which was baked at 200 °C for 12 hours and then pumped down to a pressure of  $10^{-8}$  torr. The ampoule was broken mechanically with a piston coupled to the chamber via bellows. A gamma ray spectrum taken with an HPGe detector positioned just outside the chamber is shown in Fig. 1. Since  $^{37}\text{Ar}$  decays by a ground-state-to-ground-state transition, no  $\gamma$ -ray lines are

<sup>†</sup>Physics Department, Montana State University.

<sup>1</sup>R. Abela *et al.*, Phys. Lett. **B 146**, 431 (1984).

<sup>2</sup>K. Schreckenbach, G. Colvin, and F.v. Feilitzsch, Phys. Lett. **B 129**, 265 (1983).

<sup>3</sup>L.A. Ahrens *et al.*, Phys. Rev. **D 31**, 2732 (1985).

expected in the spectrum. The dominant feature of the spectrum is the continuous internal bremsstrahlung (IB) radiation which has an endpoint energy of 813.8 keV (the  $Q_{EC}$  value of the  $^{37}\text{Ar}$  decay). Otherwise, the most prominent line is the 1460-keV  $^{40}\text{K}$  line due to room background. Since the IB intensity per  $K$  capture in  $^{37}\text{Ar}$  is known to be  $(5.2 \pm 1.3) \times 10^{-4}$ , we can deduce from the spectrum shown Fig. 1 the fraction of radioactive contaminants, if any, in the Ar source. Specifically, we have searched for  $^{42}\text{Ar}$  by looking for the 1525-keV line which would arise from its decay chain. We can place an upper limit on the decay rate of  $^{42}\text{Ar}$  of  $10^{-8}$  of the  $^{37}\text{Ar}$  decay rate. The other long lived Ar isotope which could conceivably be present is  $^{39}\text{Ar}$  ( $t_{1/2} = 269$  yr). There are no  $\gamma$ -ray lines which are associated with its decay and hence its presence cannot be deduced from the spectrum shown in Fig. 1; however, based on the maximum fraction of  $^{38}\text{Ar}$  contained in the  $^{36}\text{Ar}$  ampoule, and on the known neutron capture cross section for the  $^{38}\text{Ar}(n, \gamma)^{39}\text{Ar}$  reaction, we estimate a maximum initial decay rate that is  $3 \times 10^{-7}$  the  $^{37}\text{Ar}$  decay rate.

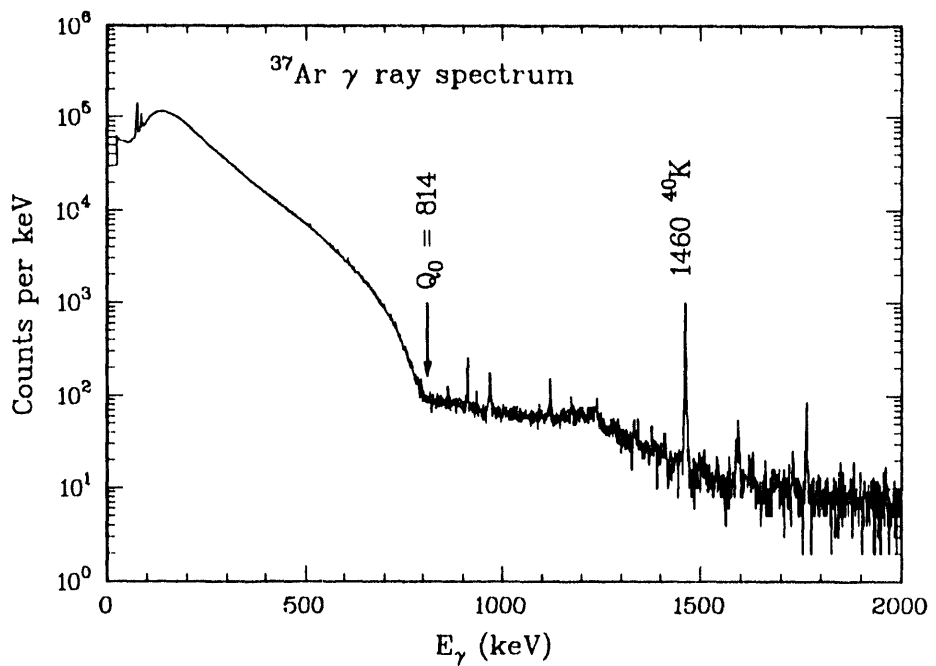


Figure 1: A four-hour spectrum of the  $^{37}\text{Ar}$  source recorded in a Gamma-X Ge detector.

The Ar gas could be bled via a leak valve into a UHV system that can be pumped down to pressures in the low  $10^{-10}$  torr range. The leak valve is sensitive enough to allow the pressure to remain in the  $10^{-10}$  torr range while the gas is being bled and hence to allow the adsorption of a single monolayer over a time period that is as long as a couple of hours, if so desired. The Ar gas was adsorbed onto a gold-coated Si(111) surface. The Au layer was evaporated onto the Si in vacuum and has a thickness of approximately 1000 Å.

The Si wafer is mounted on a cold finger which is cooled by a  ${}^4\text{He}$  cryo pump. The lowest temperature we have measured at the Si wafer is 14 K, which is slightly higher than the design temperature of 10 K of the cryo pump. We have determined that the temperature at which the first layer of Ar gets adsorbed is about 34 K and that subsequent layers get adsorbed at 24 K or lower.

We are currently utilizing microchannel plates (MCPs) to detect the Cl ions and a Channeltron detector to detect the Auger electrons. Each of the detectors has retarding screens at its entrance that serve to stop particles with energies lower than a certain value from entering the detector. Fig. 2 shows a schematic diagram of the biases applied to the screens in front of the MCPs and to the front face of the first MCP. To retard positive ions a positive potential  $V$  is applied to the middle screen. This potential reflects ions with energy  $E < qV$ , where  $q$  is the charge of the ion.

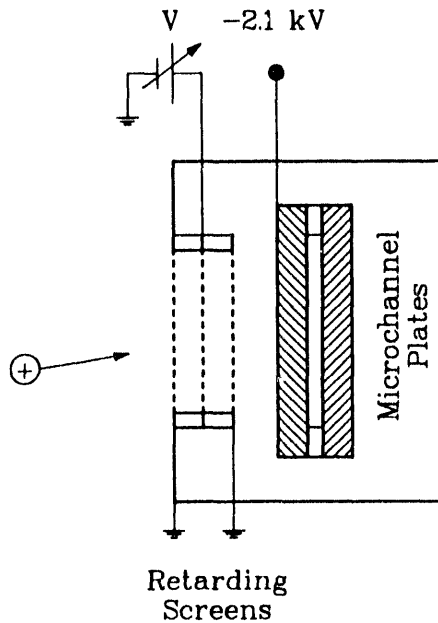


Figure 2: Schematic diagram of the electrical connections for positive ion detection in the MCP.

Fig. 3 shows the number of counts as a function of the retarding potential, recorded in the MCP over a total period of 6.5 days. Fig. 3(a) shows the number of counts when the Si wafer (with the Ar adsorbed on it) is facing the MCP, while Fig. 3(b) shows a background spectrum, taken with the sample physically blocked from the view of the MCP. Fig. 3(a) shows a clear increase in the counts below a retarding potential of 10 V, which is the potential needed to reflect singly charged  ${}^{37}\text{Cl}$  ions following EC decay ( $E = 9.54\text{ eV}$ ).

The count rate appears to be flat in the range  $\approx 5 - 8$  V and then increases again below 5 V, which is what one would expect for doubly charged Cl ions of energy 9.54 eV (which would require a stopping potential of 4.8 V). The background count rate does not account for all the counts we observe above 10 V. We believe the counts above 10 V are due to the  $KLL$  Auger electrons which are emitted following the  $K$ -electron capture of  $^{37}\text{Ar}$ . The maximum energy of the  $KLL$  Augers is 2.6 keV; the potential difference of 2.1 kV between the channel plate and the last grid (Fig. 2), which is designed to accelerate the positive Cl ions to energies high enough to initiate the electron multiplication process in the MCP, is not sufficient to prevent electrons of energy greater than 2.1 keV from reaching the plate.

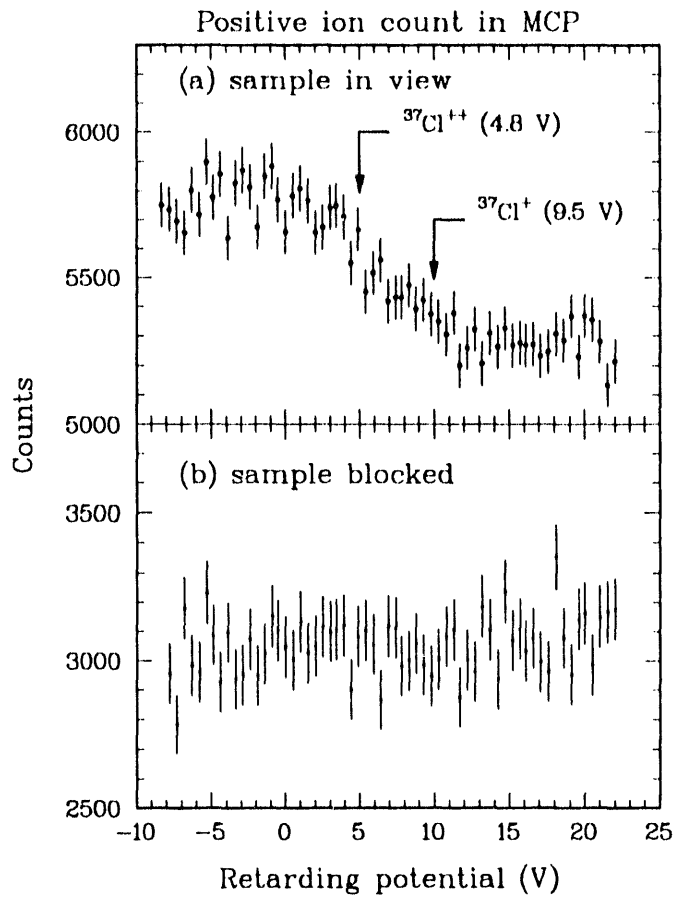


Figure 3: Positive ion count in the MCP, recorded for 6.5 d, as a function of the retarding potential. (a) Spectrum recorded with the  $^{37}\text{Ar}$  sample in view; (b) spectrum with the sample blocked.

Fig. 4 shows the number of electron counts in the Channeltron as a function of the retarding potential. As in Fig. 3, each point represents the number of electrons with energy  $E > eV$  (*i.e.*, the electron energy distribution is the negative derivative of the spectrum shown in the figure). The increase below 200 V is due to the Cl *LMM* Augers (centroid energy of 163 eV). The counts above 200 V are due to *KLL* Augers; the retarding screens we are currently employing do not support voltages higher than about 1500 V, so we are unable to see the expected drop in counts above 2.6 kV, the potential needed to stop the highest energy *KLL* Augers. The ambient background rate in the detector (lower set of data in Fig. 4) is quite acceptable for the coincidence experiments we plan to carry out.

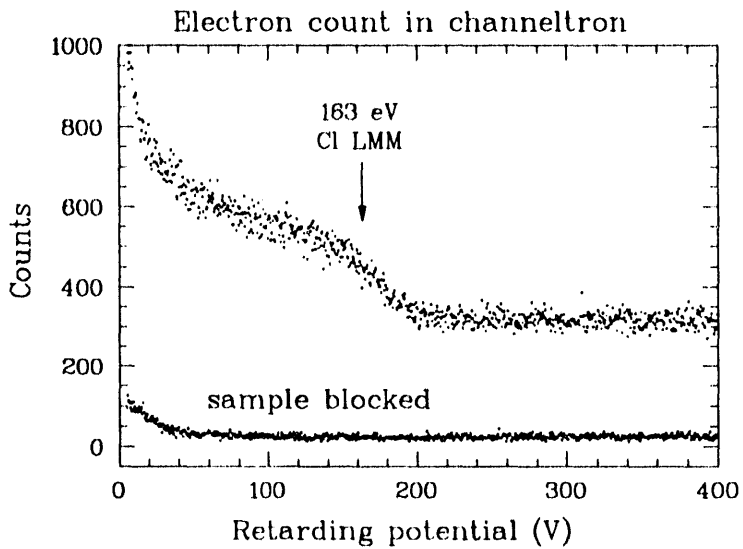


Figure 4: Electron count in the Channeltron as a function of the retarding potential. The upper spectrum is recorded with the  $^{37}\text{Ar}$  sample in view, the lower spectrum with the sample blocked.

We have also observed coincidences between the *KLL* and *LMM* Auger electrons. The coincidences were recorded between signals from two Channeltrons, one whose screens had a retarding potential of 100 V, and the other with screens having a retarding potential of 240 V.

To summarize, we have made considerable progress towards measuring the recoil velocity of Cl ions following EC decay of  $^{37}\text{Ar}$ . We have obtained a high purity  $^{37}\text{Ar}$  sample, adsorbed 1-2 monolayers of it on a gold-coated Si wafer cooled to 20 K and have strong evidence that we have detected, in singles, the recoiling  $^{37}\text{Cl}$  ions and the Auger electrons associated with the  $^{37}\text{Ar}$  decay. We are currently waiting for a fresh  $^{37}\text{Ar}$  sample, and will try to measure coincidences between the recoils and the Augers next.

## A Monte Carlo Simulation of the Electron Capture Decay of $^{37}\text{Ar}$ with an Admixture of Massive Neutrinos

D.W. Bardayan,<sup>†</sup> M.M. Hindi, R.L. Kozub, S.J. Robinson, R. Avci,<sup>‡</sup>  
G.J. Lapeyre,<sup>‡</sup> and Lin Zhu<sup>‡</sup>

We are conducting a study of the recoil velocities of  $^{37}\text{Cl}$  following the electron capture decay of  $^{37}\text{Ar}$ .<sup>1</sup> An atomic monolayer of  $^{37}\text{Ar}$  will be deposited on a cooled silicon crystal in an ultrahigh vacuum system. The  $^{37}\text{Ar}$  atom decays by electron capture into a  $^{37}\text{Cl}$  atom and a neutrino. Energy and momentum conservation then dictate that the  $^{37}\text{Cl}$  atom recoils with a fixed energy of 9.54 eV. If a 200 keV neutrino is emitted, the recoil energy is reduced to 8.955 eV. This recoil energy can be measured by starting a time-to-amplitude (TAC) converter on x rays or Auger electrons emitted in filling the hole left in the atom after electron capture, and stopped by detecting the positively charged recoiling  $^{37}\text{Cl}$  ion after it travels a distance of several centimeters. If a heavy neutrino is emitted, then there should be two peaks in this time spectrum corresponding to the two different neutrinos emitted.

There are many effects which could broaden these peaks in the time spectrum and make it difficult to resolve them. There is thermal broadening due to the motion of the  $^{37}\text{Ar}$  atom before it decays. There is broadening due to the variations of the electric field inside the Channeltron detectors. Finally, there is broadening due to the variations in the direction of motion of the Auger electrons after Auger emission. A Monte Carlo simulation was done which included all of these effects to see if the two time peaks could be resolved. Another question which we hoped to answer was whether we needed to reduce the surface temperature from 40 to 10 K to reduce the thermal broadening.

In the simulation the  $^{37}\text{Cl}$  detector is 6 cm away from the Ar source. The Auger detector which starts the TAC is at a 45 degree angle to the other detector and is located 5 cm away from the source. Both detectors are Channeltron detectors which have an active surface that is conical in shape. The base of the cone is 8 mm wide, and the height is 1 cm tall.

---

<sup>‡</sup>Physics Department, Montana State University

<sup>†</sup>TTU Student

<sup>1</sup>See the previous report on  $^{37}\text{Ar}$  for motivation.

The idea behind the Monte Carlo simulation was as follows: The recoiling  $^{37}\text{Cl}$  ion was given a velocity of magnitude appropriate for either a heavy or massless neutrino. The direction of recoil was random but in the general direction of the detector. A thermal velocity was then added to this recoil velocity. The magnitude was given by the Maxwell-Boltzman distribution of velocities at a given temperature, and the direction was random. Next an Auger recoil velocity was added. The magnitude was fixed since the K Auger electron has an energy of 2.6 keV. This Auger electron will be detected at a 45 degree angle, so the direction of the Auger recoil is in the opposite direction of the detector. A schematic of this process is shown in Figure 1. After the  $^{37}\text{Cl}$  is given its velocity, we then followed the ion's motion in time until it was detected. Electric field variations in the detector were taken into account.

The results are shown in Figures 2 and 3. Here we have included the recoil of the  $^{37}\text{Cl}$  ion after a 0.27 keV L-Auger electron was emitted. This L-Auger electron is not detected in Figure 2, but it is detected in the Auger detector in Figure 3. From these spectra it seems to be easier to resolve the two peaks if the L-Auger electron is detected. Furthermore, it appears to be necessary to reduce the surface temperature of the silicon crystal to 10 K. The effects of variations in the electric field inside the detector were much smaller than all other effects.

Some future modifications are necessary to better simulate the actual experiment: 1) a molecular dynamics calculation will have to be done to understand what effect interactions with the silicon crystal have on the recoil velocity of the  $^{37}\text{Cl}$  ion, and 2) the fact that the  $^{37}\text{Ar}$  is not a point source but is distributed over a small area also will have to be taken into account.

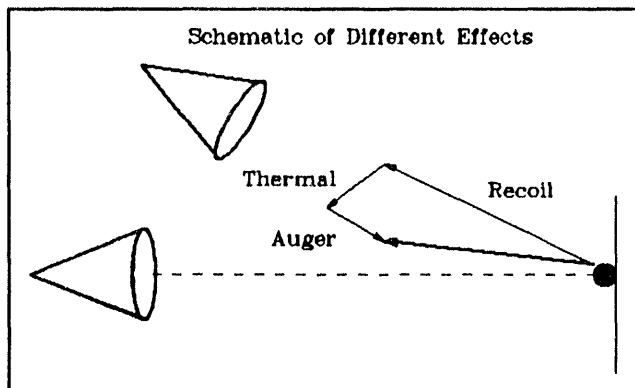


Figure 1: Schematic of the process by which the  $^{37}\text{Cl}$  ion is given its initial velocity.

Figure 2: Histogram of times when only the K-Auger electron is detected.

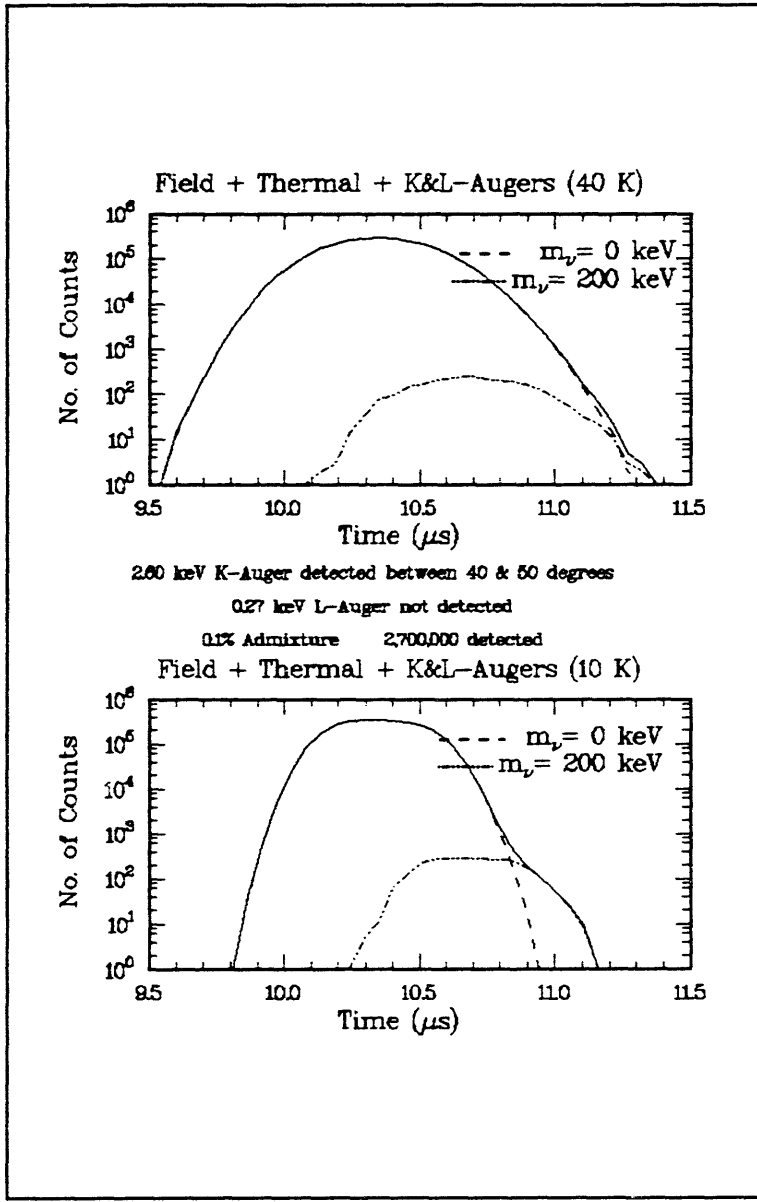
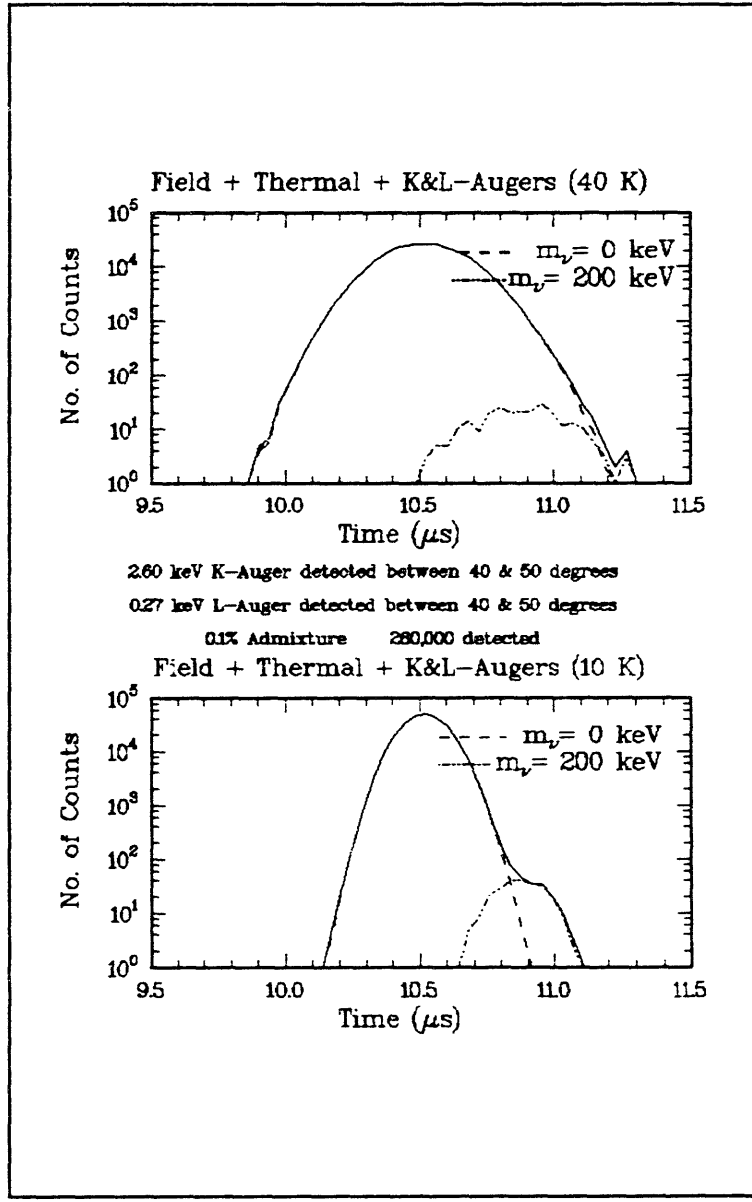


Figure 3: Histogram of times when both the K- and L-Auger electrons are detected.



## Search for 17-keV Neutrinos in the Internal Bremsstrahlung Spectrum of $^{125}\text{I}$

M. M. Hindi, R. L. Kozub, J. G. Parker\* and S. J. Robinson

In last year's progress report<sup>1</sup> we described an experiment to search for 17-keV neutrinos in the internal bremsstrahlung spectrum of  $^{125}\text{I}$ . We have counted the source for an additional period of 61 d and the background for an additional period of 7 d. We have conducted a preliminary analysis of both sets of data and report here the results for the second set. The two sets have similar statistics, but the second set should give more reliable results because (1) pileup in the second set is smaller by a factor of two (the count rate at the start of the second set was  $650 \text{ s}^{-1}$ , vs  $1300 \text{ s}^{-1}$  for the first set), (2) the  $^{126}\text{I}$  contaminant ( $t_{1/2} = 13.0 \text{ d}$ ), had decayed away to a negligible level.

Figure 1 shows the raw  $^{125}\text{I}$  spectrum (with electronic pileup rejection) for ADC 1, compressed 8 channels to a bin, along with the properly normalized background,  $^{137}\text{Cs}$  (contaminant), and residual pileup spectra. The background spectrum represents a total counting period of 17.2 d and has been multiplied by a factor of 3.54, the ratio of counting times for the  $^{125}\text{I}$  and background spectra. This ratio is in reasonable agreement with the ratio of the photo peak counts of the 185.7-keV and 238.6-keV lines in the two spectra ( $3.31 \pm 0.28$ ). We will eventually investigate the effect of a systematic change of  $\pm 10\%$  in the background normalization factor. The  $^{137}\text{Cs}$  spectrum was measured using a standard calibration source. The normalization factor was obtained by normalizing the calibration spectrum to the  $^{125}\text{I}$  spectrum, after background subtraction, in the energy region 290–311 keV. This normalization factor (0.077) agrees very well with the normalization factor of  $0.078 \pm 0.003$ , based on the yield of the 661-keV line, measured in a  $91 \text{ cm}^3$  coaxial HPGe detector.

The shape of the residual pileup spectrum was computed by convoluting the raw  $^{125}\text{I}$  spectrum with itself, subtracting the result from the raw  $^{125}\text{I}$  spectrum to obtain a first order pileup-corrected spectrum, and then repeating the process using the new  $^{125}\text{I}$  spectrum, until the process has converged. The pileup spectrum was normalized by fitting it to the  $^{125}\text{I}$  spectrum in the region above the endpoint, after background and  $^{137}\text{Cs}$  subtraction.

The energy calibration of the spectrum was determined using  $^{109}\text{Cd}$ ,  $^{57}\text{Co}$  and  $^{133}\text{Ba}$  sources. The variation in the centroids of the peaks in the calibration spectra was less than 20 eV over the time of measurement. The response function of the detector was determined from the  $^{109}\text{Cd}$  and  $^{57}\text{Co}$  lines. The relative efficiency was determined using

\*TTU student

<sup>1</sup>R.L. Kozub and M.M. Hindi, *Progress Report on Research in Nuclear Physics, 1991–1992*, (DOE/ER/40314-6), 6 (1992).

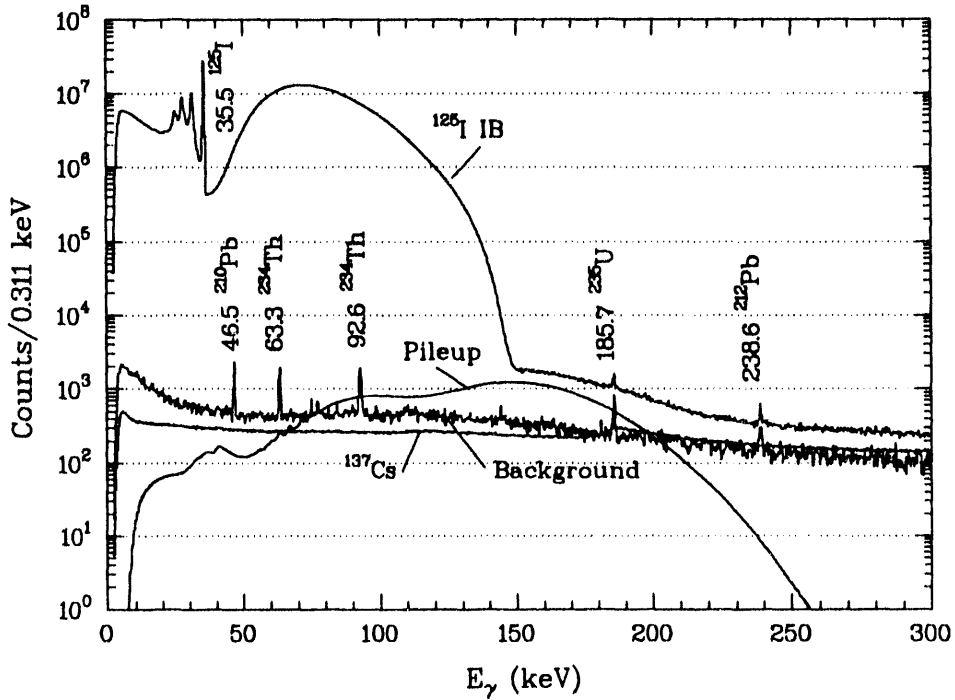


Figure 1: Spectra of the  $^{125}\text{I}$  source and of the scaled background,  $^{137}\text{Cs}$  contaminant and pileup.  $\gamma$ -ray energies are given in keV.

a  $^{182}\text{Ta}$  source. To avoid summing, the  $^{182}\text{Ta}$  spectra were taken with the source at a distance of 8 cm from the normal position of the  $^{125}\text{I}$  source (0.8 cm from the detector). The possible variation in the relative efficiency as a function of distance from the detector was examined by looking at the ratio of yields of lines from  $^{109}\text{Cd}$  and  $^{57}\text{Co}$  as a function of distance. The change in the ratio of the 88-keV-to-136-keV lines, as the source was moved from 0.8 cm to 8 cm, was found to be less than 3%.

After subtracting the room background, the contribution of the  $^{137}\text{Cs}$  contaminant, and the residual pileup, the spectra were compressed to 8 channels per bin [0.311 keV per bin for the spectrum collected via the first amplifier-ADC combination (ADC/AMP 1), and 0.266 keV per bin for the spectrum collected with the second amplifier-ADC combination (ADC/AMP 2)]. The region from 120–150.5 keV was fit with a theoretical shape that was convoluted with the measured response function and integrated over the width of a bin. The theoretical shape we used consisted of the incoherent sum of IBEC spectra associated with the emission of two neutrinos, one with zero mass and emission probability  $\cos^2 \theta$  and the other with mass  $m_\nu$  and emission probability  $\sin^2 \theta$ :

$$\frac{d\omega(E)}{dE} = \frac{d\omega(E, 0)}{dE} \cos^2 \theta + \frac{d\omega(E, m_\nu)}{dE} \sin^2 \theta. \quad (1)$$

The IBEC spectral shape as a function of the photon energy  $E$  in the case of emission of

a neutrino of mass  $m$  is given by:

$$\frac{d\omega(E, m)}{dE} = \sum_n \left[ \frac{d\omega_{ns}(E, m)}{dE} + \sum_j \frac{d\omega_{np_j}(E, m)}{dE} \right], \quad (2)$$

with  $n$  running over all the atomic shells and  $j$  over the two possible values of the total angular momentum for  $p$  orbitals:  $1/2$  and  $3/2$ . The spectral shape which we used for  $ns$ -IBEC is<sup>2</sup>

$$\frac{d\omega_{ns}(E, m)}{dE} \sim |\psi_{ns}(0)|^2 E (Q_0 - B_{ns} - E) [(Q_0 - B_{ns} - E)^2 - m^2 c^4]^{1/2}, \quad (3)$$

where  $\psi_{ns}(0)$  is the value of the wavefunction at the origin of an electron in the  $ns$  orbital in the parent atom,  $Q_0$  is the energy of the transition, and  $B_{ns}$  is the binding energy of an electron in the  $ns$  orbital in the daughter atom. For the  $np$ -IBEC we use<sup>2</sup>

$$\frac{d\omega_{np_j}(E, m)}{dE} \sim \Gamma_j |M_{np}(E)|^2 E (Q_0 - B_{np_j} - E) [(Q_0 - B_{np_j} - E)^2 - m^2 c^4]^{1/2}. \quad (4)$$

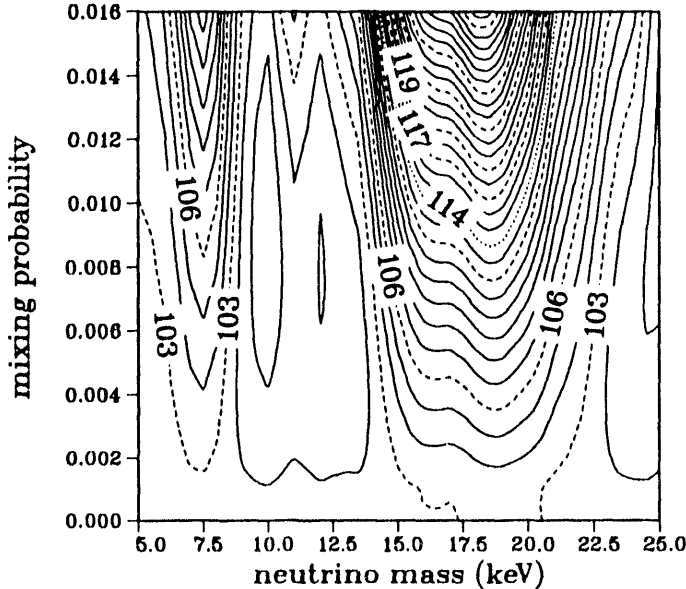
Here  $\Gamma_j$  is a weighing factor taken as 0.5 for  $j = 1/2$  and 1 for  $j = 3/2$ ;  $M_{np}(E)$  is the dipole matrix element for  $p$ -IB,<sup>2</sup> and  $B_{np_j}$  the binding energy for an electron in the  $np_j$  orbital of the daughter atom. We have evaluated  $M_{np}(E)$  in the same manner as Borge *et al.*,<sup>2</sup> and used, as they did, non-relativistic Roothan-Hartree-Fock atomic wavefunctions.

Since the IB theory does not reproduce the absolute magnitude of the IB spectra as well as it does the shapes, we allow in the fitting procedure the possibility of including an independent scaling parameter for each of the  $ns$  and  $np$  IB components. To reduce the number of free parameters, we have restricted the fitting region to 120–150.5 keV; therefore the  $1s$  component, which has an endpoint of 118.7 keV, does not enter the fit. The difference in endpoints between the  $s$  and  $p$  components for a given  $n$  is not sufficient to enable an independent normalization of each in the fit; *i.e.*, if one allowed the normalization of both the  $2s$  and  $2p$  components (or the  $3p$  and  $3s$  components) to vary simultaneously one would get large and correlated errors on the normalization of the  $s$  and  $p$  components. Also, since the contribution of IB from shells with  $n > 3$  is small over most of the fitting region and contributes independently only over the last 0.8 keV of the spectrum, no attempt was made to scale the contribution of shells with  $n > 3$  independently. Therefore, in the final fits presented here, only the ratio of the  $3p$  to  $2p$  IB components was allowed to vary freely. To absorb possible deviations of the theoretical shape from the true spectral shape, and to account for any residual smooth variations in the efficiency, response function, and pileup subtraction that we have used, we multiply the spectrum by a shape factor of the form  $P(E) = [1 + a_1(E - 151 \text{ keV}) + a_2(E - 151 \text{ keV})^2]$ , where the parameters  $a_1$  and  $a_2$  are allowed to vary freely. Thus, in the fitting procedure five parameters were allowed to vary freely: an overall normalization parameter  $C$ , the ratio  $A$  of the  $3p$  to  $2p$  IB components,  $Q_0$ ,  $a_1$ , and  $a_2$ .

---

<sup>2</sup>M.J.G. Borge *et al.*, Phys. Scr. **34**, 591 (1986), and references therein.

To search for massive neutrinos a least-squares fit of the data to the shape described above was conducted. For a given value of the pair  $(m_\nu, \sin^2 \theta)$  the  $\chi^2$ -value was minimized by allowing the parameters  $C$ ,  $A$ ,  $Q_0$ ,  $a_1$ , and  $a_2$  to vary freely. This procedure was conducted for the data collected through both ADC/AMP 1 (0.311 keV per bin, 98 data points) and ADC/AMP 2 (0.266 keV per bin, 114 data points). Figure 2 shows the  $\chi^2$  contours for the ADC/AMP 1 data set; Fig. 3 shows the same  $\chi^2$  values, plotted as a three-dimensional surface. The  $\chi^2$  value for a single massless neutrino is 102.5. The absolute minimum of  $\chi^2$  in the region searched is 100.8 [at  $(m_\nu = 12.0 \text{ keV}, \sin^2 \theta = 0.8\%)$ ]. According to statistical theory,<sup>2</sup> if the null hypothesis holds, *i.e.*, if the data are well represented by a fit with one massless neutrino, then the difference in the  $\chi^2$  value between a fit with a single massless neutrino and a fit with two additional parameters ( $m_\nu$  and  $\sin^2 \theta$ ) should itself be distributed like a  $\chi^2$  distribution with two degrees of freedom. Therefore, if the two additional parameters are superfluous, the expected improvement in the  $\chi^2$  is 2 units. Hence the local minimum at  $(m_\nu = 12.0 \text{ keV}, \sin^2 \theta = 0.8\%)$ , which is lower by 1.7 units than the  $\chi^2$  for a single massless neutrino, is not statistically significant. The  $\chi^2$  for a 17 keV neutrino with a mixing probability of 1% is 114.4, *i.e.*, 13.5 units higher than the minimum, and hence can be excluded at the 99.9% confidence level. The  $\chi^2$  for a 17 keV neutrino with a mixing probability of 0.8%, the lowest central value reported in the literature, is 9.9 units higher than the minimum and hence can be excluded at the 99.3% confidence level. The limit on a 17 keV neutrino is 0.5%, at the 95% confidence level.



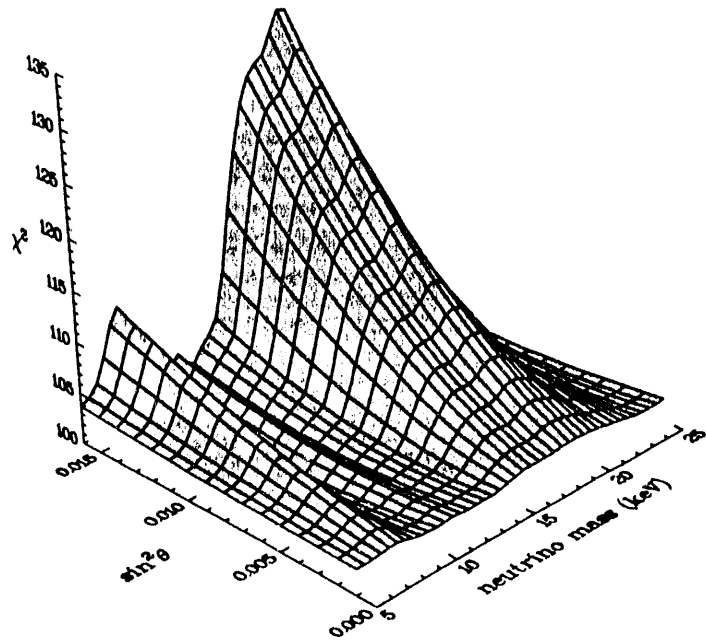


Figure 3: Surface plot of  $\chi^2$  values shown in Fig. 2.

To test for the possible dependence of the above results on amplifier or ADC nonlinearities, the data routed through AMP/ADC 2 (0.266 keV per bin, 114 data points) were also analyzed in the same manner. The corresponding results are: for a massless neutrino  $\chi^2 = 111.5$ ; absolute local minimum of  $\chi^2 = 111$  at ( $m_\nu = 13.6$  keV,  $\sin^2 \theta = 0.4\%$ ); the  $\chi^2$  for a 17 keV neutrino with a mixing probability of 1% is 121.9, and hence is excluded at the 99.6% confidence level; the  $\chi^2$  for a 17 keV neutrino with a mixing probability of 0.8% is 118.6, and hence is excluded at the 97.8% confidence level. The limit on a 17 keV neutrino is 0.7%, at the 95% confidence level.

Figures 4(a) and 4(b) show, respectively for ADC/AMP 2 and ADC/AMP 1, the ratio of the data to the fit for massless neutrinos; the solid curves show the ratio of the fit for a 17 keV neutrino with a mixing fraction of 1% to that obtained with  $m_\nu = 0$ . The fit parameters are listed in Table 1. The agreement in the values of the parameters extracted from the two AMP/ADC combinations indicates that the effects of integral nonlinearities are negligible; the slight difference in the statistical significance of the fits indicates that there are some residual differential nonlinearities, but that these are not large enough to negate our main conclusion: the hypothesis of a 17-keV neutrino admixed with the electron neutrino with a mixing fraction of 0.8% is rejected at a confidence level  $> 97.8\%$ .

We have recently obtained from Tihomir Surić the codes for calculating IB spectra

using relativistic self-consistent field methods<sup>3</sup> and we will reanalyze our data using wavefunctions calculated from these codes. We will also continue to investigate the effect of systematics on our conclusions.

Table 1: Fitting results.

	ADC/AMP 1		ADC/AMP 2	
	$m_\nu = 0$	$m_\nu = 17 \text{ keV}$	$m_\nu = 0$	$m_\nu = 17 \text{ keV}$
	$\sin^2 \theta = 1\%$			
Fitted region	120.0 – 150.0 keV			
Data points	98	98	114	114
$\chi^2$	102.5	114.3	111.5	121.9
$Q_{\text{EC}}^a$ (keV)	$185.91 \pm 0.06$	$185.83 \pm 0.06$	$185.94 \pm 0.06$	$185.86 \pm 0.06$
$3p$ to $2p$ ratio	$1.78 \pm 0.16$	$1.92 \pm 0.16$	$1.73 \pm 0.16$	$1.87 \pm 0.16$
$a_1$ (MeV $^{-1}$ )	$-6.6 \pm 1.2$	$-4.7 \pm 1.1$	$-7.2 \pm 1.2$	$-5.3 \pm 1.1$
$a_2$ (MeV $^{-2}$ )	$-0.23 \pm 0.18$	$-0.12 \pm 0.17$	$-0.31 \pm 0.18$	$-0.19 \pm 0.17$

<sup>a</sup>  $Q_{\text{EC}} = Q_0 + 35.49 \text{ keV}$

<sup>3</sup>T. Surić, R. Horvat, and K. Pisk, Phys. Rev. C47, 47 (1993).

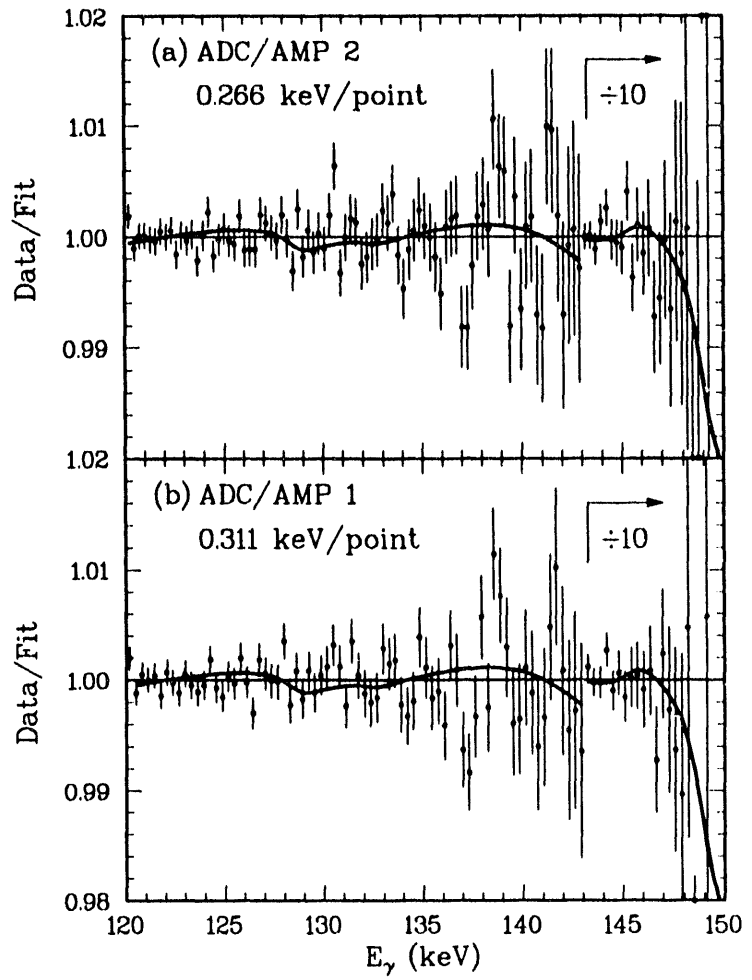


Figure 4: (a) Ratio of experimental data to the theoretical fit with a single massless neutrino. The solid curve is the ratio of the theoretical fit obtained with  $m_\nu = 17$  keV,  $\sin^2 \theta = 1\%$  to the theoretical fit with  $m_\nu = 0$ . The data are those obtained through ADC/AMP 2. (b) Same as (a) for data obtained through ADC/AMP 1.

## Production Cross Sections from the Bombardment of Natural Mo with Protons

D.W. Bardayan,<sup>†</sup> M.M. Hindi, Y. Chan,<sup>‡</sup> M.T.F. da Cruz,<sup>‡</sup>\* A. Garcia,<sup>‡</sup>  
R.-M. Larimer,<sup>‡</sup> K.T. Lesko,<sup>‡</sup> E.B. Norman,<sup>‡</sup> R.G. Stokstad,<sup>‡</sup>  
F.E. Wietfeldt,<sup>‡</sup> I. Žlimen<sup>‡</sup>○, and A.F. Barghouty<sup>†</sup>

In the laboratory,  $^{91}\text{Nb}$  decays by electron capture (EC) with a 680 year half-life (Fig. 1). However, as a high energy cosmic ray, it would be stripped of its atomic electrons and would be able to undergo only  $\beta^+$  decay. Hence the cosmic-ray half-life of  $^{91}\text{Nb}$  depends on its  $\beta^+$  partial half-life. This partial half-life has been measured to be  $(8.8 \pm 1.9)$  million years.<sup>1</sup> Since its half-life is on the order of millions of years, then  $^{91}\text{Nb}$  could serve as another cosmic-ray chronometer and as a probe of models of the interstellar medium and of the propagation of this secondary component of cosmic-rays.<sup>2</sup> However, several problems must be overcome before  $^{91}\text{Nb}$  can be used as a cosmic-ray chronometer. First of all, in the cosmic rays there will be present three niobium isotopes:  $^{91,92,93}\text{Nb}$ .  $^{93}\text{Nb}$  is stable, is produced in stars via the s- and r-neutron capture processes, and will be injected into the cosmic rays.  $^{91,92}\text{Nb}$  are expected to be present in the cosmic rays only as products of spallation reactions of molybdenum and heavier elements on interstellar hydrogen.  $^{92}\text{Nb}$  is an electron-capture-only nuclide which will become essentially stable as a bare cosmic-ray nucleus, but  $^{91}\text{Nb}$  will have a half-life of approximately 9 million years. Thus, in order to determine the age of these medium weight cosmic-ray nuclei, one will need to measure: 1) the isotopic composition of cosmic-ray niobium, and 2) the relative  $^{91}\text{Nb}$  and  $^{92}\text{Nb}$  production cross sections from proton-induced spallation reactions on abundant heavier elements. With this purpose in mind, we set out to measure these relative production cross sections, and we also measured many others in the process.

A natural Mo target was irradiated at the LBL Bevatron with 1.85 GeV protons. The

<sup>†</sup>TTU student

<sup>‡</sup>Nuclear Science Division, Lawrence Berkeley Laboratory, Berkeley, California 94720

\*Permanent address: Physics Institute, University of São Paulo, São Paulo, Brazil

<sup>§</sup>Physics Department, University of California, Berkeley, California 94720

<sup>○</sup>On leave from Rugjer Bošković Institute, Zagreb, Croatia

<sup>¶</sup>Physics Department, Roanoke College, Salem, Virginia 24153

<sup>†</sup>M.M. Hindi, et al., in print Phys. Rev. C

<sup>‡</sup>R. Silberberg and C.H. Tsao, Phys. Rep. 191, 351 (1990) and references therein.

Mo target was a disk of diameter 3.05 cm and had a thickness of 0.666 cm. The irradiation was performed with the target in air, with the Mo slab assembled in a stack, together with Polycast Acrylic sheets (polymethyl methacrylate,  $[C_3O_2H_8]_n$ ). These plastic targets served as monitors of the integrated beam current, through the production of  $^{11}C$ , from the C and O contents of the plastic.<sup>3,4</sup> The bombardment time was one hour and the integrated current was 60 nC. Following the irradiation, the target was  $\gamma$ -counted with a coaxial HPGe detector inside a lead shielding 2 inches thick. The active volume of the detector was  $\sim 100$  cm<sup>3</sup>. The target was at a distance of 8.3 cm from the detector. Three different length time bins were used for counting: 5-minute bins during the first hour, 1-hour bins during the next 24 hours, and then several 6-hour bins. The target was then counted again 49 days later for a period of two days in order to specifically look for the decay of  $^{91m}Nb$  ( $t_{1/2}=60.9$  days).

The relative efficiency of our detector was measured from the decay of  $^{88}Nb$ ,  $^{90}Nb$ ,  $^{96}Nb$ , and  $^{86}Y$  in our target. This takes into account absorption by the source since it was determined directly from the spectra of the target. The absolute efficiency of our detector was determined at an energy of  $\sim 1300$  keV by counting a calibrated  $^{152}Eu$  source in the same setup with the target removed. The corrections to the efficiency due to sum-coincidence effects were found to be less than one percent by using the KORSUM program.<sup>5</sup>

By measuring the decay of a certain isotope as a function of time in our spectra, we were able to deduce the number of atoms of that isotope which were present at the end of irradiation. We were then able to determine the production cross-section of that isotope. Since, however, some isotopes can be made both directly and by the creation of a parent which then feeds the daughter isotope, some of the cross-sections are quoted only as effective cross-sections. In other cases, we were not able to determine a cross-section for an isotope for a variety of reasons such as its half-life was too short or there were no gamma-rays associated with its decay. In the case of  $^{91}Nb$  and  $^{92}Nb$ , the effective cross-section is all we need since it does not matter in the cosmic rays how it is made. The values of the cross-sections are shown in Table I along with theoretical calculations by Silberberg and Tsao.<sup>2</sup>

---

<sup>3</sup>A.R. Smith, J.B. McCaslin, J.C. Hill and J.P. Vary, Phys. Rev. C28, 1614 (1983).

<sup>4</sup>D.L. Olson et al., Phys. Rev. C28, 1602 (1983).

<sup>5</sup>K. Debertin and R.G. Helmer, *Gamma- and X-Ray Spectrometry with Semiconductor Detectors*, North-Holland, 1988.

TABLE I. Effective cross-sections for 1.85 GeV protons on Mo

	Z	A <sup>a</sup>	Effective $\sigma$ (mb) <sup>b</sup>	Theoretical $\sigma$ (mb) <sup>d</sup>
Mo	42	90	4.6 $\pm$ 0.1	5.3
	42	93m	3.51 $\pm$ 0.08 <sup>c</sup>	14.8
Nb	41	88	3.51 $\pm$ 0.09	15.5
	41	89m	24.9 $\pm$ 1.1	22.3
	41	90	30.3 $\pm$ 0.7 <sup>c</sup>	23.7
	41	91m	18. $\pm$ 3.	33.4
	41	92m	13.6 $\pm$ 0.5 <sup>c</sup>	20.5
	41	96	11.5 $\pm$ 0.3 <sup>c</sup>	7.7
	41	97	8.7 $\pm$ 0.3	3.6
	40	86	8.4 $\pm$ 0.3	22.5
Zr	40	89	14.7 $\pm$ 1.7 <sup>c</sup>	20.6
	39	84	6.52 $\pm$ 0.14	8.8
Y	39	85	7.6 $\pm$ 0.2	11.9
	39	86	16.1 $\pm$ 0.5	11.0
	39	87	44. $\pm$ 1.	31.0
	39	90	2.94 $\pm$ 0.07	2.8
	38	80	7.9 $\pm$ 0.3	2.4
Sr	38	81	3.4 $\pm$ 0.2	5.2
	38	83	18.6 $\pm$ 0.6	16.5
	37	78	1.49 $\pm$ 0.13	2.2
Rb	37	79	4.74 $\pm$ 0.18	7.0
	37	81	19.1 $\pm$ 0.5	12.9
	37	82m	10.7 $\pm$ 0.2 <sup>c</sup>	7.4
	37	84m	2.24 $\pm$ 0.10	1.4
	36	76	2.5 $\pm$ 0.2	4.0
Kr	36	77	4.17 $\pm$ 0.13	7.5
	36	79	12.4 $\pm$ 0.7 <sup>c</sup>	10.2

Br	35	74m	2.48 $\pm$ 0.07	3.2
	35	75	7.9 $\pm$ 0.2	9.4
	35	76	10.1 $\pm$ 0.9 <sup>c</sup>	9.8
	35	77	4.17 $\pm$ 0.13	7.5

---



---

<sup>a</sup>"m" identifies the state as being a meta-stable state.

<sup>b</sup>There is a 10% error in the overall normalization of the cross-sections which is not included.

<sup>c</sup>Direct production cross-section.

<sup>d</sup>The theoretical effective cross-section was found by summing the theoretical cross-sections of the parents and the daughter where the cross-sections of the parents were multiplied by the percentage of the time they decay to the daughter.

### Figures

Fig. 1. The decay scheme of  $^{91}\text{Nb}$  (level energies are not to scale).

Fig. 2. Three typical spectra of the irradiated Mo target in the three different length time bins.

Fig. 3. A density plot showing the production cross-sections of the products of the irradiation.

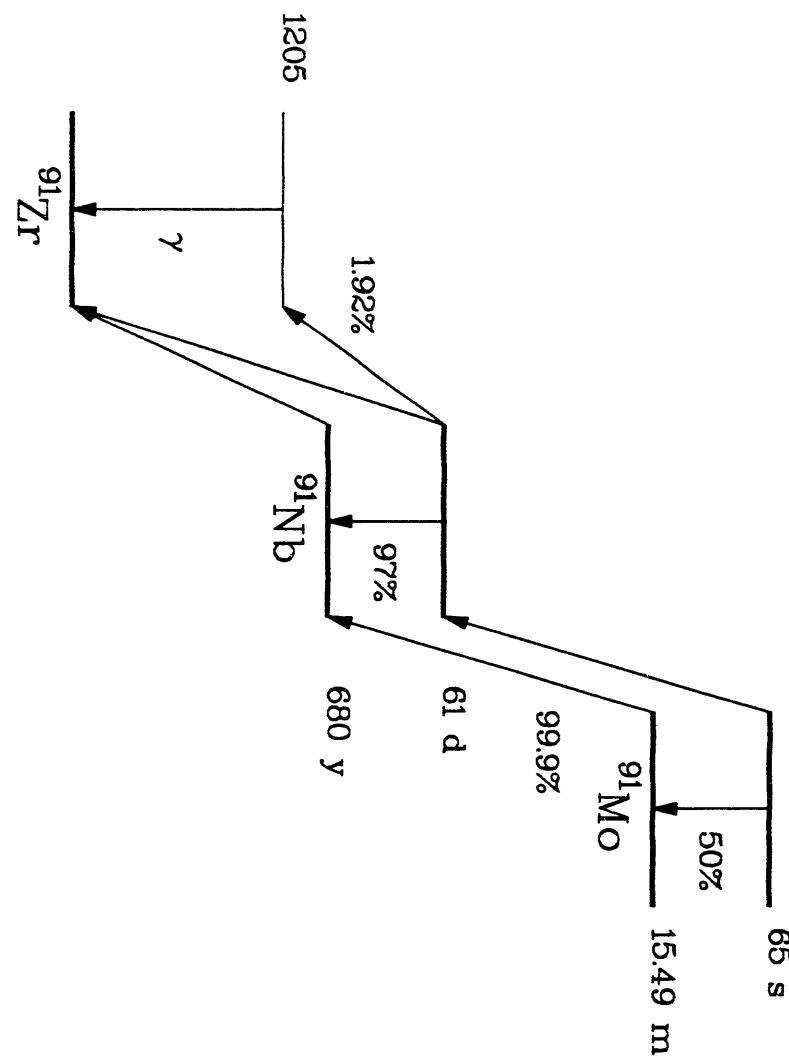


Figure 1

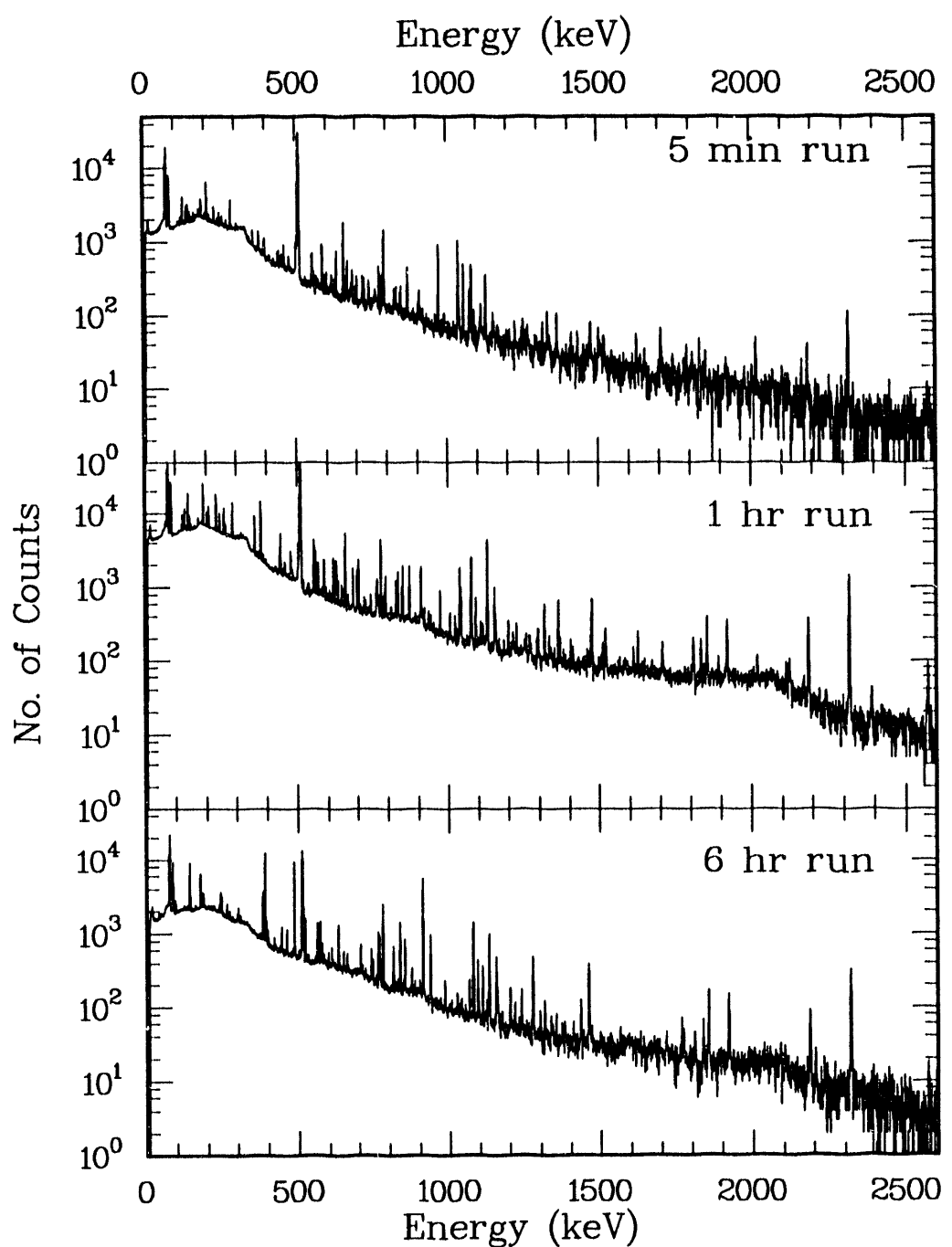


Figure 2

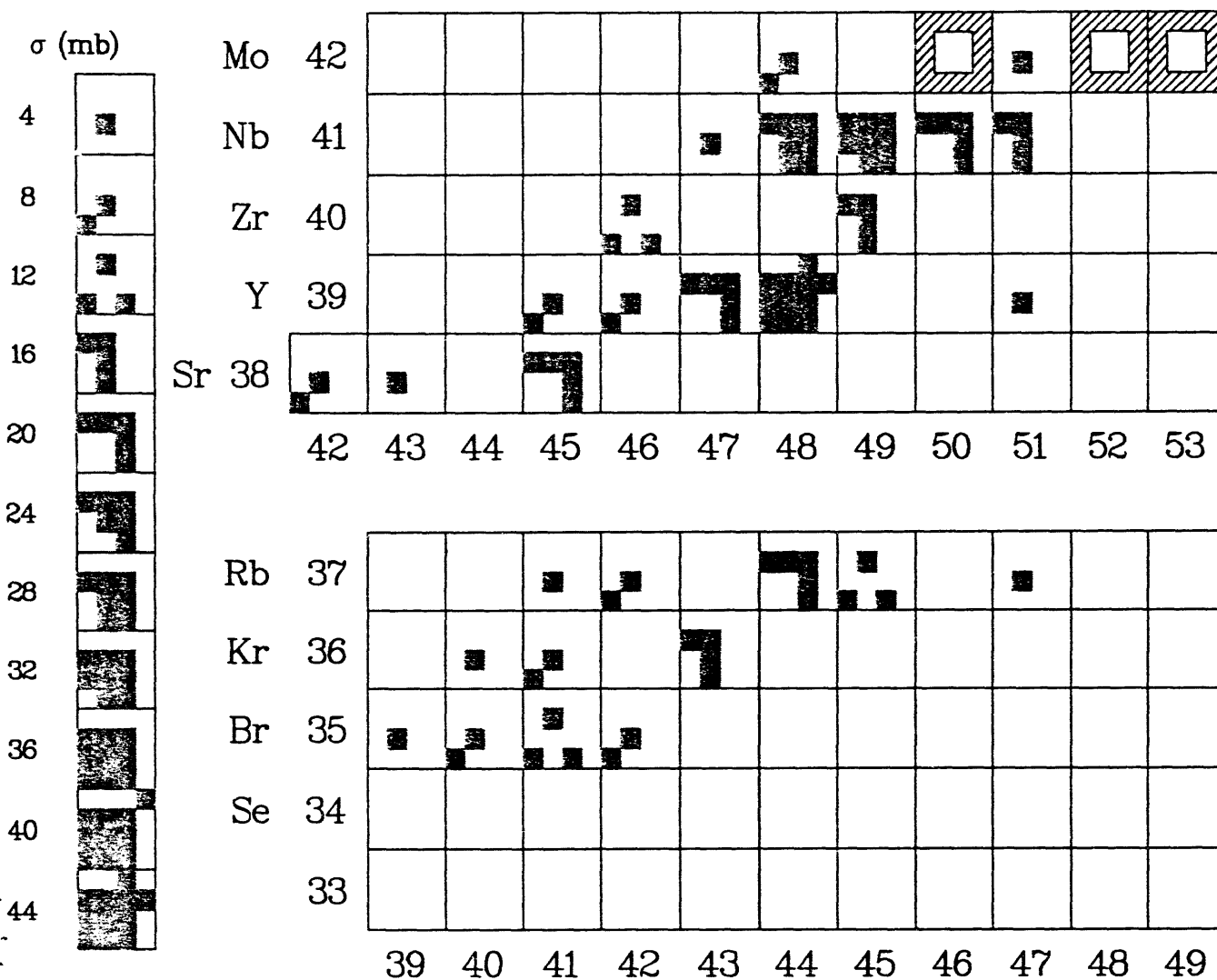


Figure 3

29

reprints removed;  
Conf Paper  
cycled separately.  
etc.

**PUBLICATIONS AND SEMINARS**  
(July 1, 1992 – June 30, 1993)

**Journal articles:**

1. “ $\beta^+$  decay and cosmic-ray half-life of  $^{91}\text{Nb}$ ”  
M. M. Hindi, Bhaskar Sur, Kristin L. Wedding, D. W. Bardayan, K. R. Czerwinski, M. T. F. da Cruz, D. C. Hoffman, R.-M. Larimer, K. T. Lesko, and Eric B. Norman, in press, *Physical Review C* **47**, 2598 (1993).
2. “Electron-Capture Decay of  $^{100}\text{Tc}$  and the Double- $\beta$  Decay of  $^{100}\text{Mo}$ ”  
A. García, Y-D Chan, M. T. F. da Cruz, R.-M. Larimer, K. T. Lesko, E. B. Norman, R. G. Stokstad, F. E. Wietfeldt, I. Žlimen, D. M. Moltz, J. Batchelder, T. J. Ognibene, M. M. Hindi, *Physical Review C* **47** 2910 (1993).
3. “Plasmon Decay into Multiple-Electron-Hole Pairs in Si(111)”  
L. Zhu, R. Avci, M. M. Hindi, G. J. Lapeyre, submitted to *Physical Review Letters*, December 1992.
4. “Evolution towards equilibration in orbiting interactions”  
B. Shiva Kumar, D. J. Blumenthal, S. V. Greene, J. T. Mitchell, D. A. Bromley, D. Shapira, J. Gomez del Campo, A. Ray, M. M. Hindi, *Physical Review C* **46**, 1946 (1992).
5. “Yrast decays in  $^{43}\text{K}$ ”  
R. L. Kozub, C. R. Bybee, M. M. Hindi, J. F. Shriner, Jr., R. Holzmann, R. V. F. Janssens, T.-L. Khoo, W. C. Ma, M. W. Drigert, U. Garg, and J. J. Kolata, *Physical Review C* **46**, 1671 (1992).
6. “Thick-target yields of iodine isotopes from proton interactions in Te, and the double- $\beta$  decays of  $^{128,130}\text{Te}$ ”  
M. T. F. da Cruz, D. W. Bardayan, Y. Chan, A. García, M. M. Hindi, R.-M. Larimer, K. T. Lesko, E. B. Norman, Della F. Rossi, R. G. Stokstad, F. E. Wietfeldt, and I. Žlimen, submitted to *Physical Review C*, May 1993.

**Papers appearing in conference proceedings:**

1. “A Massive Neutrino in Nuclear Beta Decay?”  
Eric B. Norman, Yuen-Dat Chan, M. T. F. da Cruz, Alejandro García, M. M. Hindi, K. T. Lesko, Ruth-Mary Larimer, Robert G. Stokstad, Bhaskar Sur, Fred E. Wietfeldt, Igor Žlimen, *Proceedings of the XXVI International Conference on High Energy Physics*, Dallas, Texas, August 6-12, 1992.
2. “A Massive Neutrino in Nuclear Beta Decay?”  
Eric B. Norman, Yuen-Dat Chan, M. T. F. da Cruz, Alejandro García, M. M. Hindi,

K. T. Lesko, Ruth-Mary Larimer, Robert G. Stokstad, Bhaskar Sur, Fred E. Wietfeldt, Igor Zlimen, Proceedings of the III International Symposium on Weak and Electromagnetic Interactions in Nuclei, Dubna, Russia, June 6-22, 1992.

3. "β+ Decay and Cosmic-ray Half-Life of  $^{91}\text{Nb}$ "

M. M. Hindi, Bhaskar Sur, Kristin L. Wedding, D. W. Bardayan, K. R. Czerwinski, M. T. F. da Cruz, D. C. Hoffman, R.-M. Larimer, K. T. Lesko, and Eric B. Norman, Paper submitted for the 23rd International Cosmic Ray Conference, Calgary, Canada, July 19-30, 1993.

4. "β+ Decay and Cosmic-ray Half-lives of  $^{143}\text{Pm}$  and  $^{144}\text{Pm}$ "

M. M. Hindi, Bhaskar Sur, A. E. Champagne, M. T. F. da Cruz, R.-M. Larimer, K. T. Lesko, and Eric B. Norman, Paper submitted for the 23rd International Cosmic Ray Conference, Calgary, Canada, July 19-30, 1993.

5. "Thick-target yields of iodine isotopes from proton interactions in Te, and the double-β decays of  $^{128,130}\text{Te}$ "

M. T. F. da Cruz, D. W. Bardayan, Y. Chan, A. García, M. M. Hindi, R.-M. Larimer, K. T. Lesko, E. B. Norman, D. F. Rossi, R. G. Stokstad, F. E. Wietfeldt, and I. Žlimen, Paper submitted for the 23rd International Cosmic Ray Conference, Calgary, Canada, July 19-30, 1993.

6. "Neutrino recoil induced desorption"

L. Zhu, M. Hindi, R. Avci, G. J. Lapeyre, R. Kozub, abstract submitted to the 40th National AVS Symposium & Topical Conference, Orlando, Florida, November 15-19, 1993.

**Abstracts:**

1. "Beta Spectrum of  $^{14}\text{C}$ "

E. B. Norman, Y. D. Chan, M. T. F. Da Cruz, A. García, E. E. Haller, W. L. Hansen, R. M. Larimer, K. T. Lesko, P. N. Luke, R. G. Stokstad, F. E. Wietfeldt, I. Žlimen, B. Sur, M. M. Hindi, Bulletin of the American Physical Society, **37**, 1286 (1992).

2. "Coincidence Measurements on Plasmon Excitations and Damping in Si(111) Substrate"

L. Zhu, R. Avci, G. J. Lapeyre, M. M. Hindi, Bulletin of the American Physical Society, **38**, 510 (1993).

**Invited talks:**

1. "The Rise and Fall of the 17-keV Neutrino"

M. M. Hindi, Invited colloquium, University of Missouri, Columbia, Missouri, November 9, 1992.

2. "Double *K*-Shell Ionization in the Electron-Capture Decays of  $^{139}\text{Ce}$  and  $^{125}\text{I}"$   
M. M. Hindi, Invited Seminar, Lawrence Berkeley Laboratory, Berkeley, California,  
January 8, 1993.

## TTU PERSONNEL

### Sources of Support

#### Principal Investigators

R. L. Kozub, Professor	TTU, DOE
M. M. Hindi, Associate Professor	TTU, DOE

#### Student Assistants

A. Altgilbers	DOE
D. Bardayan	DOE
B. Faircloth	DOE
P. Miočinović	DOE

#### Secretary/Account Clerk

G. J. Julian, CPS	TTU
-------------------	-----

#### Other Nuclear Physics Faculty

S. Ayik, Professor	TTU, DOE
K. Kumar, University Professor	TTU
D. P. Murdock, Assistant Professor	TTU, IU
S. J. Robinson, Assistant Professor	TTU, ORAU
P. B. Semmes, Associate Professor	TTU, DOE
J. F. Shriner, Jr., Associate Professor	TTU, DOE, ORAU
J. C. Wells, Jr., Professor	TTU, ORAU

DOE = Department of Energy

IU = Indiana University

ORAU = Oak Ridge Associated Universities

TTU = Tennessee Technological University

# DATA

四  
五  
六  
七  
八

13/46

The image consists of three separate panels arranged vertically. The top panel is a black rectangle containing a white central rectangle, with two black rectangles on either side of the white rectangle. The middle panel is a large black rectangle with a diagonal white line from bottom-left to top-right. The bottom panel is a large black rectangle with a white, rounded rectangular shape centered within it.

